Supplementary Data

Snai2 maintains bone marrow niche cells by repressing osteopontin expression

Qiaozhi Wei, Fumio Nakahara, Noboru Asada, Dachuan Zhang, Xin Gao, Chunliang Xu, Alan Alfieri, N. Patrik Brodin, Samuel E. Zimmerman, Jessica C. Mar, Chandan Guha, Wenjun Guo and Paul S. Frenette

Ruth L. and David S. Gottesman Institute for Stem Cell and Regenerative Medicine Research, Department of Cell Biology, Department of Radiation Oncology, Department of Systems and Computational Biology, Department of Epidemiology and Population Health, Department of Pathology, Department of Urology, Department of Medicine, Albert Einstein College of Medicine, Bronx, New York 10461, USA.

Figure S1 (related to Figures 1 and 2)

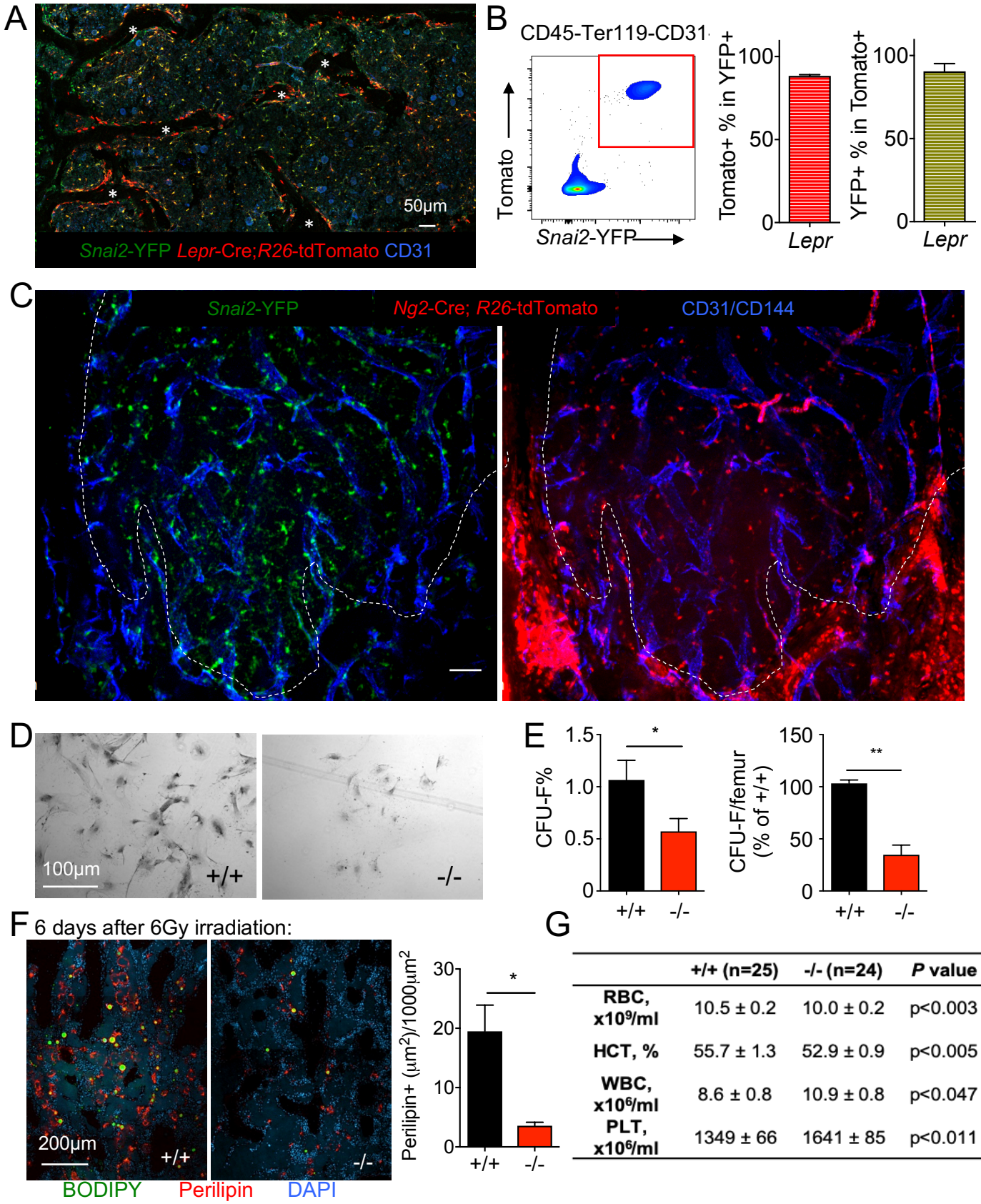

Supplemental Figure 1 (related to Figures 1 and 2). *Snai2* is expressed and required in bone marrow mesenchymal niche cells. (A) Representative immunofluorescence image of a sternum section from *Snai2*-YFP; *Lepr*-Cre; *R26*-tdTomato mice stained with anti-GFP and CD31 antibodies. Scale bar=50μm. * denotes trabeculae. **(B)** Representative FACS plot of $CD45^{-}$ $Ter119^{-}$ $CD31^{-}$ BM cells and quantifications showing nearly complete overlap of *Snai2*-YFP and *Lepr*-Cre; *R26*-tdTomato expression. **(C)** Additional fluorescence images of whole-mount sternums from *Snai2*-YFP; *Ng2*-Cre; *R26*-tdTomato mice as in Figure 1A. Scale bar=50μm. **(D)** Representative bright-field images of colony-forming unit-fibroblast (CFU-F) formed by sorted $Snai2^{+/+}$ and $Snai2^{-/-}$ BM MSCs. **(E)** CFU-F forming efficiency of $Snai2^{+/+}$ and $Snai2^{-/-}$ BM MSCs and CFU-F from femurs of $Snai2^{+/+}$ and $Snai2^{-/-}$ mice (n=6 biological samples from 3 independent experiments). **(F)** Representative immunofluorescence images from frozen sections and quantifications of $BODIPY^{+}$ $Perilipin^{+}$ adipocytes in control and $Snai2^{-/-}$ femurs 6 days after 6 Gy irradiation. **(G)** Red blood cell (RBC), hematocrit (HCT), white blood cell (WBC), and platelet (PLT) assessment of steady state $Snai2^{+/+}$ and $Snai2^{-/-}$ (-/-) mice. Data are shown as mean ± s.e.m. *p< 0.05, **p< 0.01 by unpaired Student's *t* test.

Figure S2 (related to Figure 3)

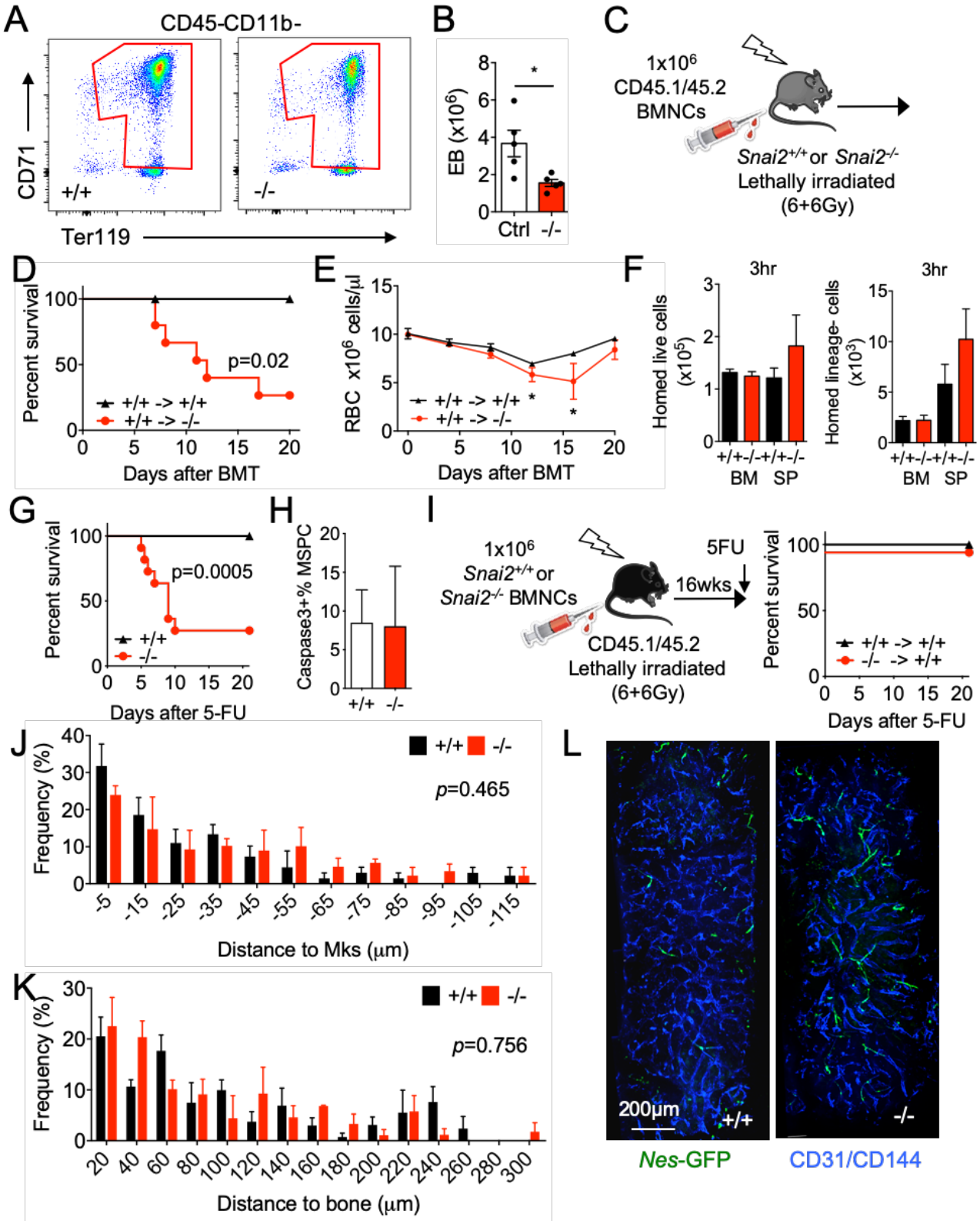

Supplemental Figure 2 (related to Figure 3). *Snai2* deletion alters hematopoiesis and the HSC niche. (A and B) Representative FACS plots (A) and quantification of erythroblast (EB) numbers (B) in femur of control (Ctrl) and *Snai2*$^{-/-}$ mice. **(C and D)** Experimental design (C) and Kaplan-Meyer survival curve (D) of *Snai2*$^{+/+}$ and *Snai2*$^{-/-}$ recipients reconstituted with wild-type donor BM cells. *p* value derived by log-

rank test (n=10 mice per group from 2 independent experiments). **(E)** RBC assessments of *Snai2*$^{+/+}$ and *Snai2*$^{-/-}$ recipients reconstituted with wild-type donor BM cells at indicated time points. **(F)** Quantification of homed live cells and Lin$^-$ cells in the BM of lethally irradiated *Snai2*$^{+/+}$ and *Snai2*$^{-/-}$ recipients 3h after the transplantation. (n=3 mice per group) **(G)** The Kaplan-Meyer survival curve of *Snai2*$^{+/+}$ and *Snai2*$^{-/-}$ mice treated with a single dose of 250 mg/kg body weight 5FU. *p* value derived by log-rank test (n=11 mice from 4 independent experiments). **(H)** Evaluation of apoptosis in *Nes*-GFP$^+$ BM MSPC population in *Snai2*$^{+/+}$ and *Snai2*$^{-/-}$ mice by cleaved Caspase3 staining 1 day after 5FU injection (n=3). **(I)**Experimental design and Kaplan-Meyer survival curve of wild-type recipients reconstituted with *Snai2*$^{+/+}$ and *Snai2*$^{-/-}$ donor BM cells that are treated with 250 mg/kg body weight 5FU. n=5 mice per group. **(J and K)** Spatial distribution of phenotypic HSCs observed *in situ* relative to megakaryocytes (Mks) (I) and bone (J). *p* value was determined by two-sample Kolmogorov-Smirnov test. **(L)** Representative immunofluorescence images of whole-mount sternums from *Snai2*$^{+/+}$ and *Snai2*$^{-/-}$ mice showing the distribution of *Nes*-GFP^{Hi} cells. Data are mean ± s.e.m. *p< 0.05 by unpaired Student's *t* test unless otherwise indicated.

Figure S3 (related to Figure 4)

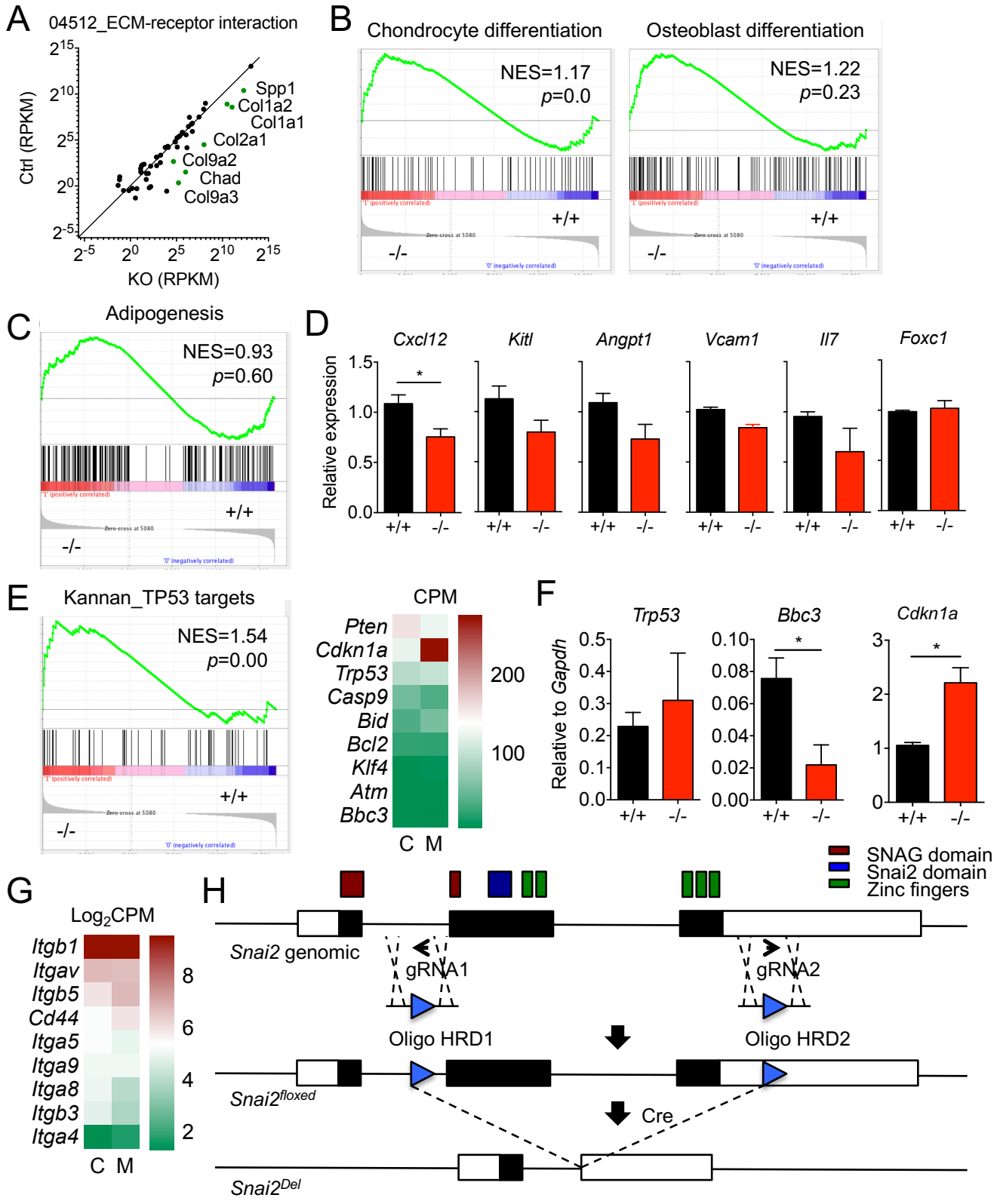

Supplemental Figure 3 (related to Figure 4). Gene expression changes in *Snai2*-deficient MSPCs. (A) RNA-seq analysis showing significantly up-regulated extracellular matrix (ECM) proteins in control (Ctrl) and *Snai2*$^{-/-}$ (KO) MSPCs. n=3 per group. **(B)** RNA-seq and Gene Set Enrichment Analysis (GSEA) enrichment plots showing enriched expression of chondrocyte and osteoblast differentiation related gene

sets in *Snai2*$^{-/-}$ BM MSPCs compared to wild type. **(C)** GSEA enrichment plot showing that adipogenesis related genes were not differentially enriched in wild-type or *Snai2*$^{-/-}$ BM MSPCs. **(D)** qRT-PCR confirmation of niche factor gene expression in wild-type and *Snai2*$^{-/-}$ MSPCs. n=3-5. *p< 0.05 by unpaired Student's *t* test. **(E)** GSEA enrichment plot and heat map showing P53 modulated gene expression in *Snai2*$^{-/-}$ BM MSPCs compared to wild type. **(F)** qRT-PCR confirmation of *Trp53, Bbc3* and *Cdkn1a* expression in wild-type and *Snai2*$^{-/-}$ MSPCs. n=3-5 biological samples. *p< 0.05 by unpaired Student's *t* test. **(G)** Heat map showing the expression of Osteopontin receptors in *Snai2*$^{-/-}$ BM MSPCs compared to wild type. **(H)** Schematic targeting strategy of *Snai2*^{floxed} allele using CRISPR/Cas9 technology. Exons are depicted by boxes with black coding regions. LoxP sites are marked as blue triangles.

Figure S4 (related to Figure 4)

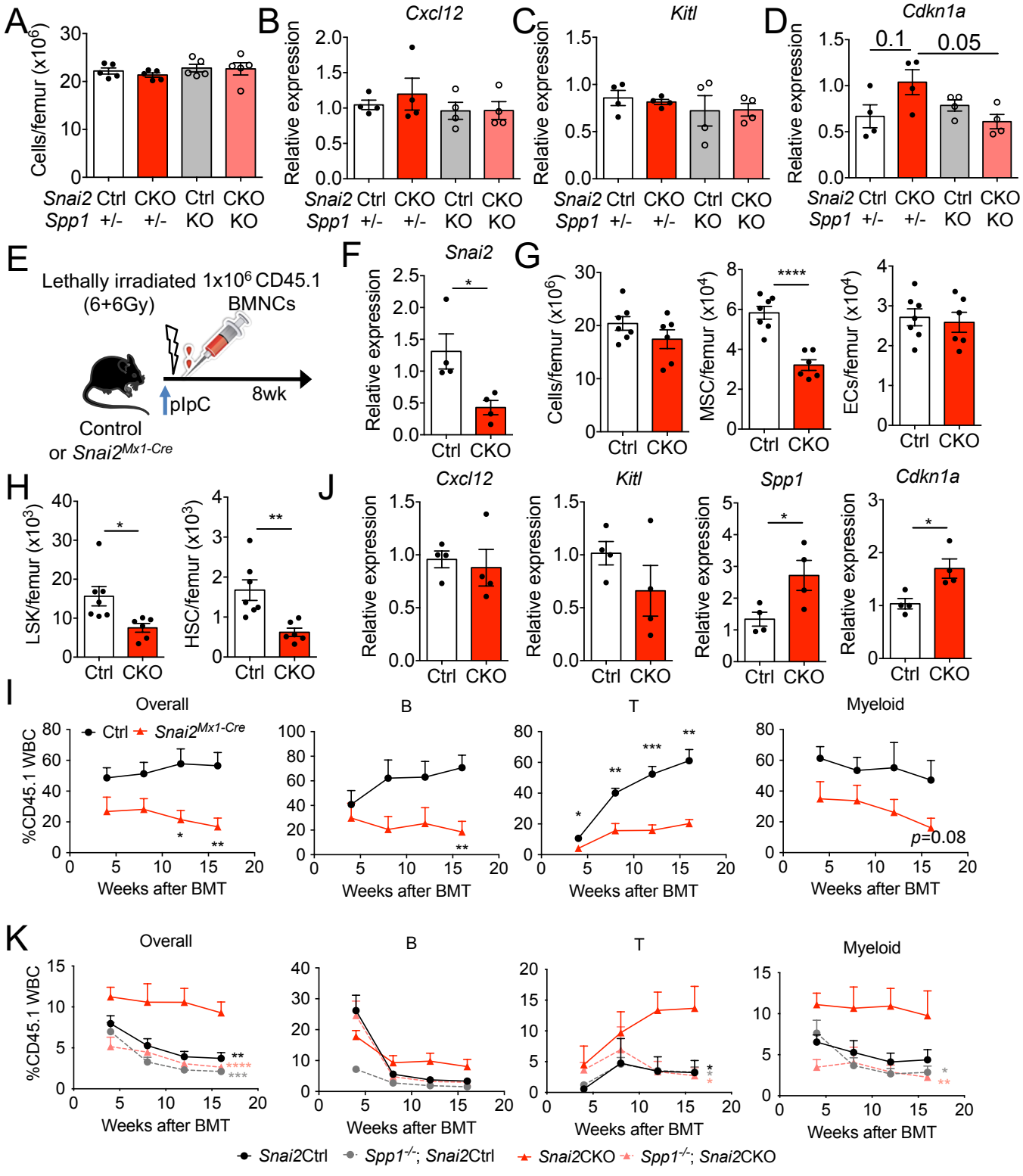

Supplemental Figure 4 (related to Figure 4). *Snai2* regulates adult BM MSPC niche via suppression of *Spp1*. (A) Quantification of BM cellularity of *Snai2*$^{Mx1\text{-}Cre}$; *Spp1*$^{-/-}$ compound knockout mice at 8 wks after pIpC injections. **(B-D)** qRT-PCR analysis of *Cxcl12* (B), *Kitl* (C) and *Cdkn1a* (D) expression in sorted BM MSCs from *Snai2*$^{Mx1\text{-}Cre}$; *Spp1*$^{-/-}$ compound knockout mice at 8wks after pIpC injections. **(E)** Experimental design of lethally irradiated control (Ctrl) and *Snai2*$^{Mx1\text{-}Cre}$ (CKO) recipients reconstituted

with wild-type (CD45.1) donor cells. **(F)** *Snai2* mRNA measured by qRT-PCR in sorted BM MSCs from control (Ctrl) and *Snai2*$^{Mx1\text{-Cre}}$ (CKO) recipients reconstituted with wild-type (CD45.1) donor cells. **(G and H)** Quantification of BM cellularity, MSC and EC numbers (G) and LSK and HSC numbers (H) in femurs of control (Ctrl) and *Snai2*$^{Mx1\text{-Cre}}$ (CKO) recipients reconstituted with wild-type (CD45.1) donor cells. **(I)** Contribution of wild-type donor BM cells (CD45.1) from control (Ctrl) and *Snai2*$^{Mx1\text{-Cre}}$ (CKO) recipients to peripheral blood after competitively transplanted with equal volume of CD45.2 competitor cells at indicated time points. n=5 mice per group. **(J)** qRT-PCR analysis of *Cxcl12*, *Kitl, Spp1* and *Cdkna1* expression in sorted BM MSPCs from control and *Snai2*$^{Mx1\text{-}Cre}$ mice at 8wks after BM transplant (n=4-7 biological samples from 2 independent experiments). **(K)** Peripheral blood analysis of donor (CD45.1)-derived leukocytes in lethally irradiated recipients transplanted with 200 purified HSCs from (I) (CD45.1) and 0.4 x 10^6 WT competitor BMNCs (CD45.2). n=4 mice per group. Significance was shown for comparisons between *Snai2*CKO and all the other groups and calculated using multiple comparisons Two-way ANOVA. All other data are shown as mean ± s.e.m. *p< 0.05, **p< 0.01, ***p<0.001 by unpaired Student's *t* test unless otherwise indicated.

Supplemental Table 1 (related to Figure 4). Ingenuity canonical pathways enriched by most down-regulated genes in *Snai2*$^{-/-}$ MSCs compared to wild type.

	Ingenuity Canonical Pathways	-log(p-value)	Ratio	Molecules
1	Granulocyte Adhesion and Diapedesis	3.20E+00	2.82E-02	CXCL16,Ppbp,PF4,Ccl7,ITGB3
2	Epithelial Adherens Junction Signaling	2.60E+00	2.74E-02	TUBB1,SNAI2,TUBA4A,ZYX
3	IL-9 Signaling	2.11E+00	5.88E-02	STAT5A,CISH
4	Integrin Signaling	2.07E+00	1.93E-02	ITGA2B,ITGA8,ZYX,ITGB3
5	P2Y Purigenic Receptor Signaling Pathway	1.95E+00	2.52E-02	ITGA2B,P2RY1,ITGB3
6	Thrombopoietin Signaling	1.71E+00	3.64E-02	STAT5A,MPL
7	Acute Phase Response Signaling	1.55E+00	1.78E-02	C3,VWF,RBP4
8	Wnt/β-catenin Signaling	1.55E+00	1.78E-02	SFRP2,SFRP1,UBC
9	Agrin Interactions at Neuromuscular Junction	1.53E+00	2.90E-02	LAMA2,ITGB3
10	JAK/Stat Signaling	1.50E+00	2.78E-02	STAT5A,CISH
11	Prostanoid Biosynthesis	1.46E+00	1.11E-01	PTGES
12	Clathrin-mediated Endocytosis Signaling	1.45E+00	1.62E-02	UBC,RBP4,ITGB3
13	RAR Activation	1.42E+00	1.58E-02	STAT5A,ADH7,RBP4
14	Calcium Transport I	1.42E+00	1.00E-01	ATP2A3
15	Role of Osteoblasts, Osteoclasts and Chondrocytes in Rheumatoid Arthritis	1.27E+00	1.37E-02	SFRP2,SFRP1,ITGB3

Supplemental Table 2 (related to Figure 4). Ingenuity canonical pathways enriched by most up-regulated genes in *Snai2*$^{-/-}$ MSCs compared to wild type.

	Ingenuity Canonical Pathways	-log(p-value)	Ratio	Molecules
1	Hepatic Fibrosis / Hepatic Stellate Cell Activation	7.08E+00	6.01E-02	COL1A2,COL1A1,IGF2,FN1,COL13A1,HGF,COL22A1,MMP13,MMP2,COL11A1,COL11A2
2	Role of Osteoblasts, Osteoclasts and Chondrocytes in Rheumatoid Arthritis	4.55E+00	4.11E-02	COL1A1,BGLAP,ITGA3,IL1RN,BMP3,MMP13,WNT4,SP7,ALPL
3	Atherosclerosis Signaling	3.58E+00	4.84E-02	COL1A2,COL1A1,IL1RN,PLA2G5,MMP13,COL11A2
4	Agranulocyte Adhesion and Diapedesis	3.38E+00	3.70E-02	ITGA3,FN1,IL1RN,MMP16,EZR,MMP13,MMP2
5	Triacylglycerol Degradation	3.19E+00	1.25E-01	LIPC,MGLL,PNPLA2
6	cAMP-mediated signaling	3.00E+00	3.20E-02	ENPP6,GRM7,P2RY14,ADRA2A,VIPR2,PKIA,PDE4B
7	Sphingomyelin Metabolism	2.86E+00	2.50E-01	SGMS2,SMPD3
8	VDR/RXR Activation	2.63E+00	5.13E-02	BGLAP,COL13A1,CDKN1A,VDR
9	Leukocyte Extravasation Signaling	2.52E+00	3.03E-02	ITGA3,MMP16,EZR,MMP13,MMP2,BMX
10	Axonal Guidance Signaling	2.40E+00	2.07E-02	ITGA3,SEMA4D,SEMA3D,BMP3,UNC5B,MMP13,WNT4,MMP2,NGF